Modeling potentiometric measurements in topological insulators including parallel channels

Seokmin Hong,[*] Vinh Diep, and Supriyo Datta[†]

School of Electrical and Computer Engineering, Purdue University, West Lafayette, Indiana 47907, USA

Yong P. Chen

Department of Physics, Purdue University, West Lafayette, Indiana 47907, USA

The discovery of spin-polarized states at the surface of three-dimensional topological insulators (TI) like Bi_2Te_3 and Bi_2Se_3 motivates intense interests in possible electrical measurements demonstrating unique signatures of these unusual states. Here we show that a three-terminal potentiometric set-up can be used to probe them by measuring the voltage change of a detecting magnet upon reversing its magnetization. We present numerical results using a nonequilibrium Green's function (NEGF)-based model to show the corresponding signal quantitatively in various transport regimes. We then provide an analytical expression for the resistance (the measured voltage difference divided by an applied current) that agrees with NEGF results well in both ballistic and diffusive limits. This expression is applicable to TI surface states, two-dimensional electrons with Rashba spin-split bands, and any combination of multiple channels, including bulk parallel states in TI, which makes it useful in analyzing experimental results.

I. INTRODUCTION

Following the discovery of spin-polarized states at the surface of three-dimensional topological insulators (TI), such as Bi_2Te_3 and Bi_2Se_3 (see, for example, Refs. [1] and [2], and references therein), there is intense interest in possible electrical measurements demonstrating unique signatures of these unusual states.[3–5] A recent interesting proposal[6] suggests that a unique signature of TI material should be a change in the conductance measured between a normal contact and a ferromagnetic (FM) contact when the magnetization of the latter is reversed.

We believe that in order to observe this effect it is important to use a multiterminal measurement in the linear response regime. Any two-terminal resistance measurement using magnetic contacts on a material described by a time-reversal invariant (TRI) Hamiltonian should obey a generalized Onsager relation of the form $R(\vec{M}) = R(-\vec{M})$ (see, for example, Refs. [7–9] and references therein), with $\vec{M}$ being a magnetization in the linear response regime. For multiterminal measurements, Onsager relation requires that $R_{ab,cd}(\vec{M}) = R_{cd,ab}(-\vec{M})$, where the first and second pair of indices are used to denote contacts to supply current and measure the voltage difference, respectively. However, there is no requirement for $R_{ab,cd}(\vec{M})$ to equal $R_{ab,cd}(-\vec{M})$. Indeed in this paper we will show how the quantity $R_{12,13}(\vec{M}) - R_{12,13}(-\vec{M})$ measured using a specific three-terminal (3T) potentiometric set-up[8] with $R_{12,13}(\vec{M}) = V(\vec{M})/I$ [Fig. 1(a)] can be related to the spin orientation of the eigenstates of the channel.

We establish this result starting from a quantitative nonequilibrium Green's function (NEGF)-based model that allows us to (1) go seamlessly from the ballistic to the diffusive limits and (2) include multiple conduction paths described by different Hamiltonians that may be in parallel with the TI channel. We will show that the numerical results from the NEGF model can

be described well by the following expression, which we will also justify using simple physical arguments:

$$[V(\vec{M}) - V(-\vec{M})]/I = R_B(\vec{p} \cdot \vec{m}), \qquad (1)$$

with

$$\vec{p} = \frac{\sum_i \sum_{v_x(\vec{k})>0} \hat{s}_i(\vec{k})\delta[E_F - \epsilon_i(\vec{k})]}{\sum_i \sum_{v_x(\vec{k})>0} \delta[E_F - \epsilon_i(\vec{k})]}, \qquad (2)$$

where $1/R_B$ is a ballistic conductance of the channel, which is given by q^2/h times the number of modes or conducting channels $\sim k_F W/\pi$ for each Fermi circle (k_F, Fermi wave number; W, width of channel) and E_F is the Fermi energy. The effective magnet polarization is represented by $P_{FM} = (G_M - G_m)/(G_M + G_m)$, which defines $\vec{m} = P_{FM}\hat{M}$, with $G_{M(m)}$ being the contact conductance for majority (minority) spins and I is the applied current along the x direction. The channel property $\vec{p}$ can be viewed as the degree of the spin polarization per unit current in the x direction and applies to arbitrary dispersion $\epsilon_i(\vec{k})$ and spin orientation $\hat{s}_i(\vec{k})$, including combinations of TI surface states (TI SS) channels and Rashba spin-orbit coupling (SOC) materials (Fig. 2) each represented by a channel index i. The quantity $\vec{p}$ provides a measure of the average spin polarization of all states with positive group velocity [$v_x(\vec{k}) = \partial \epsilon/\hbar \partial k_x > 0$], which for TRI material is the negative of the average spin polarization of states with negative group velocity. As a result there is no spin polarization at equilibrium, but there is a current induced spin polarization, as discussed in the literature (see, for example, Refs. [10] and [11]). If we reverse the current, I, the measured voltage, $V(\vec{M}) - V(-\vec{M})$ will also reverse.

Two points: (1) The above expression is valid both in the ballistic and diffusive limits, which, we will show, is supported by NEGF results (Fig. 3).
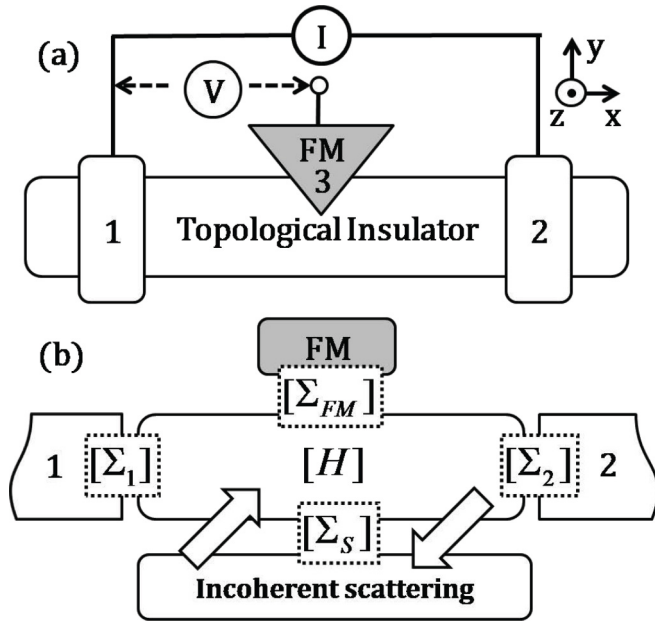
FIG. 1. (a) Schematic view of three-terminal potentiometric set-up with two current probes (1 and 2) and one FM voltage probe (3). (b) NEGF model: Hamiltonian (H) with four different self energies. Σ_1 and Σ_2 are used to model contacts 1 and 2. Σ_{FM} is used to model a FM contact. Σ_S is responsible for incoherent processes in the diffusive limit.

(2) To the best of our knowledge, this type of signal has not been observed in TI yet but it has been experimentally confirmed in Rashba SOC materials.[12] The expression given here applied to Rashba channel is consistent with the one that has been used in the past to describe experimental results quantitatively.[13]

In order to ensure that the potentiometric set-up measure a channel property ($\vec{p}$) in a minimally invasive way, it is advisable to use a weakly coupled contact, which also enhances the signal as seen in experimental work on Rashba SOC materials.[14,15]
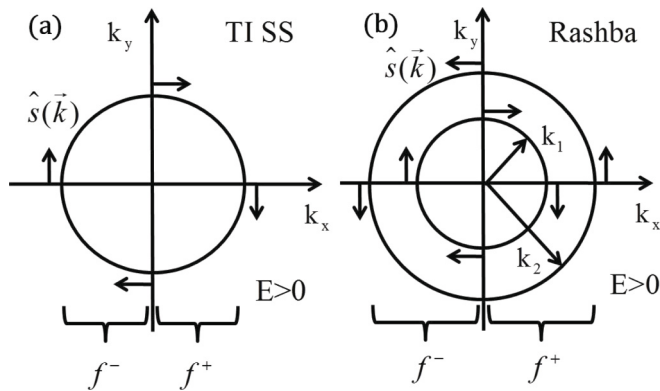

FIG. 2. Schematic view of Fermi circles at a given energy for (a) TI SS and (b) Rashba materials from a given dispersion relation $\epsilon_i(\vec{k})$ with positive $\hbar v_F$ and α. The occupation factors for positive and negative propagating states are given by f^+ and f^-, respectively. Arrows are unit vectors representing the spin direction $\hat{s}_i(\vec{k})$ of each eigenstate.
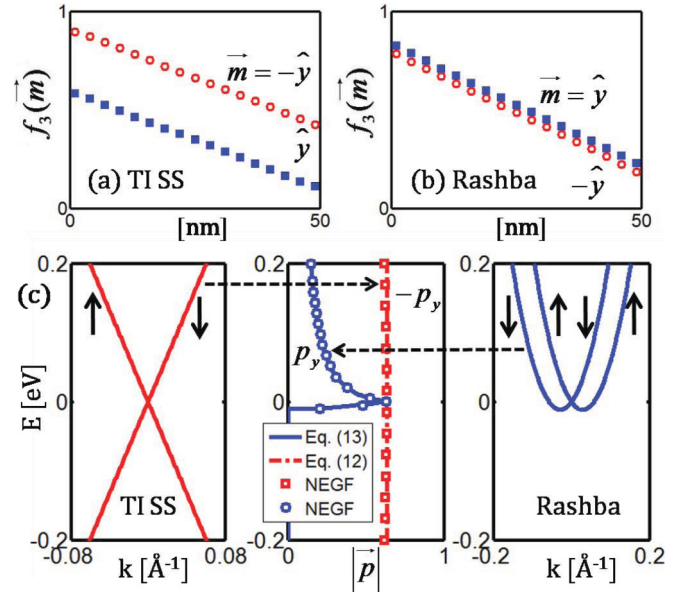

FIG. 3. (Color online) Results of NEGF and simple Eqs. (12) and (13). Occupation factor [$f_3(\vec{m})$] along the length of the channel when there is a charge current in the diffusive limit (spin randomizing) for the case of (a) TI SS and (b) Rashba channel at $E_F = 0.2$ eV with $d_m = 10^{-3}$ eV^2, $a = 5$ Å, width= 50 nm. Two cases of $\vec{m}$ (= $\hat{y}$, $-\hat{y}$) are plotted. (c) The magnitude of $\vec{p}$ between TI SS and Rashba channel as a function of energy with their dispersion relations. The NEGF result in (c) assumed a ballistic transport and periodic boundary condition along the width direction. Parameters: $\hbar v_F = 3.3$ eVÅ, $m = 0.28 m_e$, $\alpha = 0.79$ eV Å.[19]

II. MODEL DESCRIPTION

For the two-dimensional (2D) top surface of a three-dimensional TI, we adopt the following model Hamiltonian on a discrete lattice:

$$H_{\text{TISS}} = \frac{\hbar v_F}{a}\{\sigma_x \sin(k_y a) - \sigma_y \sin(k_x a) - \sigma_z[\cos(k_x a) + \cos(k_y a) - 2]\}, \quad (3)$$

where the $\vec{\sigma}s$ are the Pauli spin matrices, a is the lattice spacing, and v_F is the Fermi velocity. The additional σ_z term is added to avoid fermion doubling problem on a discrete lattice (see Ref. 16 and references therein). Although this term breaks time-reversal symmetry, it is smaller than the first two terms by a factor (ka) around $k = 0$ and we have checked that all numerical results presented here are not affected if we change a or the sign of the σ_z term.

For 2D Rashba SOC materials we use the standard form for H:

$$H_{\text{Rashba}} = \frac{\hbar^2}{2m}(k_x^2 + k_y^2)I_2 + \alpha(\sigma_x k_y - \sigma_y k_x), \quad (4)$$

where I_2 is 2 by 2 identity matrix and α is a Rashba SOC strength.

The sign of $(\hat{s} \times \vec{k})_z$ for a given Fermi circle depends on whether $\hat{z}$ is chosen as the outward or inward normal to the surface. We have chosen it as the outward normal, which makes α in Eq. (4) and $\hbar v_F$ in Eq. (3) positive, based on the experimental results.[20,21]

We model the two contacts 1 and 2 as semi-infinite left and right contacts [Fig. 1(b)] and their self-energies are described by $\Sigma_{1(2)} = \tau_{1(2)} g_s \tau_{1(2)}^\dagger$, where τ is a coupling matrix between the contact and the channel and g_s is the surface Green's function of each contact. Contact 3 is modeled with $\Sigma_{\text{FM}} = -i\gamma/2(I_2 + \vec{m} \cdot \vec{\sigma}) \otimes I_w$, where we use a value of $\gamma \ll \hbar v_F/a$ to simulate a weakly coupled probe. γ represents the strength of the coupling of the contact and I_w is an identity matrix whose size is same as the width of the channel with $\otimes$ a tensor product.

The incoherent scattering is included through self energies Σ_s in the self-consistent Born approximation. We assume isotropic momentum randomizing scattering along with two types of spin scatterings. Following the notations in Ref. 17, the momentum randomizing scattering is described by

$$\left[\Sigma_s, \Sigma_s^{\text{in}}\right]_{ij} = d_m \delta_{ij} \delta_{ik} \delta_{jl} [G, G^n]_{kl}, \tag{5}$$

where i, j, k, and l are real space indices. The spin-preserving and spin-randomizing scattering[17] are described by

$$\left[\Sigma_s, \Sigma_s^{\text{in}}\right]_{ab} = \delta_{ac} \delta_{bd} [G, G^n]_{cd}, \tag{6}$$

and

$$\left[\Sigma_s, \Sigma_s^{\text{in}}\right]_{ab} = (\vec{\sigma}_{ac} \cdot \vec{\sigma}_{db})[G, G^n]_{cd}, \tag{7}$$

respectively, where a, b, c, and d are used to indicate spin indices.

The charge current I between contact 1 and 2 is calculated assuming $f_1 = 1$ and $f_2 = 0$, where f_j is the occupation factor for contact j. The value of f_3 of a FM contact is a quantity of interest for subsequent discussions. For coherent transport it is common to write $I_i \sim \sum_j \overline{T}_{ij}(f_i - f_j)$, obtaining $\overline{T}_{ij}$ from Trace$[\Gamma_i G \Gamma_j G^\dagger]$ and then solve for $I_1 = -I_2 = I$ and f_3 assuming $f_1 = 1$, $f_2 = 0$, and $I_3 = 0$.[18] However, with incoherent scattering present there is no simple expression for $\overline{T}_{ij}$ and we evaluate these coefficients numerically using $\overline{T}_{ij} = -\partial I_i / \partial f_j$.

III. RESULTS

The NEGF method described in the previous section is quite general, but we focus here on a weakly coupled FM contact that does not perturb the channel properties appreciably. By setting $I = 0$ in the NEGF equation[18] for current $[I \sim (\text{Trace}[\Gamma A]f - \text{Trace}[\Gamma G^n])]$, we can write f for the given probe as Trace$[\Gamma G^n]$/Trace$[\Gamma A]$ in the limit of $\gamma \to 0$. For a given energy E_F we first plot the occupation factor of contact 3 [$f_3(\vec{m})$] for two cases of $\vec{m}(= \hat{y}, -\hat{y})$ by continuously moving it point by point along the current flow direction. As shown in Figs. 3(a) and 3(b) for TI SS and Rashba channels, with nonzero slopes when spin randomizing scattering processes are included in the channel. The slope of each line is proportional to the magnitude of d_m [see Eq. (5)] and can be related to the conventional ohmic drop due to momentum relaxation processes.[18] When we compare f_3 with two opposite magnet directions $\hat{y}$ and $-\hat{y}$, there is a noticeable splitting between them, which is uniform along the channel, and this is true for both ballistic and diffusive transport limits with spin preserving and spin randomizing scattering. In the small bias and low-temperature limit NEGF

results at a single energy can be related to the experimentally measurable quantities using the following expression:

$$\frac{V(\vec{m}) - V(-\vec{m})}{I} = \frac{1}{(q^2/h)\overline{T}(E)} \frac{f_3(\vec{m}) - f_3(-\vec{m})}{f_1 - f_2}, \tag{8}$$

obtained by combining $f_3(\vec{m}) - f_3(-\vec{m}) = (-\partial f_0/\partial E)[\mu_3(\vec{m}) - \mu_3(-\vec{m})]$, with $I = (q/h)\overline{T}(E)(\mu_1 - \mu_2)$, μ_j being the chemical potential of contact j and f_0, the Fermi function in equilibrium. This resistance value is, in general, energy dependent but is relatively independent of whether we are in the ballistic or diffusive limits. Figure 3(c) shows the values of $\vec{p}$ deduced from the numerically calculated $[V(\vec{m}) - V(-\vec{m})]/I$, using Eq. (1), which are labeled "NEGF." These agree well with the lines obtained from the analytical expressions in Eq. (2), which we will now justify.

IV. DISCUSSION

The occupation factor for the FM contact, which draws no net charge current, is given by

$$f_3(\vec{m}) = \frac{\sum_i \sum_{\vec{k}} f(\vec{k})[1 + \vec{m} \cdot \hat{s}_i(\vec{k})]\delta[E - \epsilon_i(\vec{k})]}{\sum_i \sum_{\vec{k}}[1 + \vec{m} \cdot \hat{s}_i(\vec{k})]\delta[E - \epsilon_i(\vec{k})]}, \tag{9}$$

assuming that the current due to each state $\vec{k}$ is $[f_3(\vec{m}) - f(\vec{k})][1 + \vec{m} \cdot \hat{s}_i(\vec{k})]$. This gives

$$f_3(\vec{m}) - f_3(-\vec{m}) = \vec{m} \cdot \frac{\sum_i \sum_{\vec{k}} f(\vec{k})\hat{s}_i(\vec{k})\delta[E - \epsilon_i(\vec{k})]}{\sum_i \sum_{\vec{k}} \delta[E - \epsilon_i(\vec{k})]/2}, \tag{10}$$

assuming $\sum_i \sum_{\vec{k}} \hat{s}_i(\vec{k})\delta[E - \epsilon_i(\vec{k})] = 0$, which is true for TRI Hamiltonian since each time reversal pair is composed of two opposite spins and group velocities $[\epsilon_i(\vec{k}, \hat{s}_i(\vec{k})) = \epsilon_i[-\vec{k}, -\hat{s}_i(\vec{k})]$. Assuming that the occupation factor $f(\vec{k})$ equals f^+, f^- for states with positive and negative group velocities, respectively, we obtain

$$\frac{f_3(\vec{m}) - f_3(-\vec{m})}{f^+ - f^-} = \vec{p} \cdot \vec{m}, \tag{11}$$

where we have made use of the fact that in TRI material the factor $\vec{p}$ defined in Eq. (2) for positive group velocity states is the negative of that for for negative group velocity states. We can recover Eq. (1) by noting that $I(E)/(f^+ - f^-)$ is same as q/h times the number of conducting channels.[18] It also suggests that the signal is relatively independent of scattering processes in the channel since the above argument is applicable to both ballistic and diffusive limits.

A. TI SS channel

We can evaluate the expression $\vec{p}$ in Eq. (2) in the case of TI SS based on, for example, $\epsilon(\vec{k}) = |\hbar v_F k|$ and $\hat{s}(\vec{k}) = \text{sgn}(\hbar v_F)(\hat{x}\sin\theta - \hat{y}\cos\theta)$ when $\epsilon > 0$ from the TI SS Hamiltonian Eq. (3) as shown in Fig. 2(a) with $\tan\theta = k_y/k_x$. Using these, one can get

$$\vec{p}(E) = \text{sgn}(\hbar v_F)(0, -2/\pi, 0). \tag{12}$$

As defined, $\vec{p}$ represents the intrinsic spin polarization of the channel of current carrying electrons and $2/\pi$ comes from an angular averaging of 2D electrons. Since $\vec{p}$ is a vector along the y axis, Eq. (1) suggests that the signal is maximum when the magnet points along the y direction in the plane of the TI SS.

B. Rashba channel

The same procedure can be applied to materials with Rashba SOC using, for example, $\epsilon(\vec{k}) = \hbar^2 k^2 / 2m \pm \alpha k$ and $\hat{s}(\vec{k}) = \text{sgn}(\alpha)(\pm\hat{x}\sin\theta \mp \hat{y}\cos\theta)$ when $\epsilon > 0$ with $\tan\theta = k_y/k_x$ from the Rashba Hamiltonian Eq. (4). Upper and lower signs represent inner and outer Fermi circles, respectively, as shown in Fig. 2(b). Following the same procedure, one can get

$$\vec{p}(E) = \text{sgn}(\alpha)\left(0, \frac{2}{\pi}\frac{k_2 - k_1}{k_2 + k_1}, 0\right)$$

$$= \text{sgn}(\alpha)\begin{cases} [0,(2/\pi)(1+2E\hbar^2/m\alpha^2)^{1/2},0], & \text{if } E \geqslant 0, \\ [0,(2/\pi)(1+2E\hbar^2/m\alpha^2)^{-1/2},0], & \text{if } E \leqslant 0, \end{cases}$$

$$(13)$$

where k_1 and k_2 are inner and outer radius of Fermi circles, respectively. Note that: (1) even Rashba channels give nonzero $\vec{p}(E)$ as demonstrated earlier [see, for example, Eqs. (12) and (13)]; (2) both Eq. (13) for Rashba and Eq. (12) for TI SS come out of the same general result stated earlier in Eq. (2). The polarization for Rashba is reduced with respect to TI SS due to the imperfect cancellation of two Fermi circles [corresponding to two different "i" in Eq. (2)]with opposite spin orientations. Similar cancellation could also occur for TI SS with multiple bands.
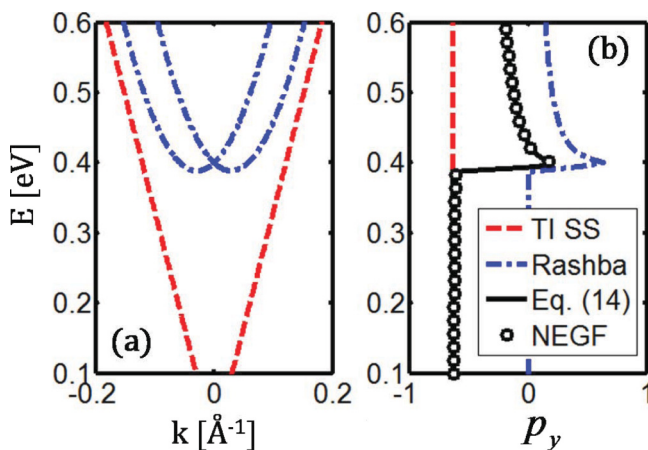

FIG. 4. (Color online) Results of NEGF and simple Eq. (14) for multiple channels. (a) Dispersion relation of TI SS (dashed line) together with Rashba bands (dashed-dotted line). (b) y component of $\vec{p}$ for the case of multiple channels (TI SS and Rashba channels) as a function of energy. The NEGF result assumed a ballistic transport and periodic boundary condition along the width direction. Parameters are the same as those described in the legend of Fig. 3(c), except for 0.4 eV shift with Rashba channel.

C. Multiple channels

The coexistence of bulk states with TI SS is one of the main obstacles to detect and identify surface states in transport measurements. When there are multiple channels with their own channel polarizations the general expression for $\vec{p}$ is given by a density of states (DOS) average of each $\vec{p}_i$ for a given channel index i,

$$\vec{p}(E) = \frac{\sum_i \vec{p}_i \text{DOS}_i}{\sum_i \text{DOS}_i}, \tag{14}$$

by noting that $\text{DOS}_i = 2\sum_{v_x(\vec{k})>0}\delta[E - \epsilon_i(\vec{k})]/A$, with A the area of 2D surface. Recent experimental reports[20,21] suggest the coexistence of Rasbha bands together with TI SS with spin orientations corresponding to positive $\hbar v_F$ and α in Eqs. (3) and (4). It implies that their contribution to p_y will have opposite signs, which could even cause a change in the sign of p_y around $E = 0.4$ eV, depending on the relative DOS of TI SS and Rashba bands as shown in Fig. 4(b). This aspect can be probed experimentally by changing E_F.

V. SUMMARY

In summary, we have shown that a three-terminal potentiometric measurement should show a change in resistance upon reversing the magnetization of a voltage detecting FM contact, and this change can be used as a quantitative measure of the channel polarization $\vec{p}$ using Eq. (2), which is applicable to TI SS and/or Rashba channels. The key result is summarized in Eqs. (1) and (2), which have been justified using an NEGF-based quantum transport model as well as simple semiclassical arguments.

APPENDIX: DERIVATIONS OF EQS. (12) AND (13)

Here we assume positive $\hbar v_F$, α, and ϵ. In the case of TI SS, there is single band given by $\epsilon(\vec{k}) = \hbar v_F k$ and $\hat{s}(\vec{k}) = \hat{x}\sin\theta - \hat{y}\cos\theta$. We start the derivation from Eq. (2).

$$\vec{p} = \frac{\sum_{v_x(\vec{k})>0}\hat{s}_i(\vec{k})\delta[E_F - \epsilon(\vec{k})]}{\sum_{v_x(\vec{k})>0}\delta[E_F - \epsilon(\vec{k})]}$$

$$= \frac{\int_{-\pi/2}^{+\pi/2} d\theta(\hat{x}\sin\theta - \hat{y}\cos\theta)\int_0^{+\infty} kdk\delta[E_F - \epsilon_i(\vec{k})]}{\int_{-\pi/2}^{+\pi/2} d\theta \int_0^{+\infty} kdk\delta[E_F - \epsilon_i(\vec{k})]}$$

$$= -\frac{2}{\pi}\hat{y},$$

which is Eq. (12).

In the case of Rashba channel, first note that we have two Fermi circles with inner and outer radius k_1 and k_2, respectively $[\epsilon_{\text{inner}}(\vec{k}) = \hbar^2 k^2/2m + \alpha k$, $\hat{s}_{\text{inner}}(\vec{k}) = \hat{x}\sin\theta - \hat{y}\cos\theta$ and $\epsilon_{\text{outer}}(\vec{k}) = \hbar^2 k^2/2m - \alpha k$, $\hat{s}_{\text{outer}}(\vec{k}) = -\hat{x}\sin\theta + \hat{y}\cos\theta]$.

For the denominator we have

$$\sum_i \sum_{v_x(\vec{k})>0} \delta[E_F - \epsilon_i(\vec{k})]$$

$$= \sum_{v_x(\vec{k})>0} \{\delta[E_F - \epsilon_{\text{inner}}(\vec{k})] + \delta[E_F - \epsilon_{\text{outer}}(\vec{k})]\}$$

$$= \frac{A}{(2\pi)^2} \int_{-\pi/2}^{+\pi/2} d\theta \int_0^{+\infty} k \, dk \left\{ \delta\left[\frac{\hbar^2}{2m}(k-k_1)(k+k_2)\right]\right.$$

$$\left. + \delta\left[\frac{\hbar^2}{2m}(k+k_1)(k-k_2)\right]\right\} = \frac{A}{(2\pi)^2}\frac{2m\pi}{\hbar^2}.$$

Based on these,

$$\vec{p} = \frac{k_1}{\pi(k_1+k_2)} \int_{-\pi/2}^{+\pi/2} d\theta (\hat{x}\sin\theta - \hat{y}\cos\theta)$$

$$+ \frac{k_2}{\pi(k_1+k_2)} \int_{-\pi/2}^{+\pi/2} d\theta (-\hat{x}\sin\theta + \hat{y}\cos\theta)$$

$$= \frac{2}{\pi}\frac{k_2-k_1}{k_2+k_1}\hat{y},$$

which is Eq. (13). The cases for negative values of $\hbar v_F$, α, or $\epsilon < 0$ can be shown similarly.

---

*hong37@purdue.edu

†datta@purdue.edu

[1] M. Z. Hasan and C. L. Kane, Rev. Mod. Phys. **82**, 3045 (2010).

[2] X.-L. Qi and S.-C. Zhang, Rev. Mod. Phys. **83**, 1057 (2011).

[3] F. Xiu, L. He, Y. Wang, L. Cheng, L.-T. Chang, M. Lang, G. Huang, X. Kou, Y. Zhou, X. Jiang, Z. Chen, J. Zou A. Shailos, and K. L. Wang, Nat. Nanotechnol. **6**, 216 (2011).

[4] J. W. McIver, D. Hsieh, H. Steinberg, P. Jarillo-Herrero, and N. Gedik, Nat. Nanotechnol. **7**, 96 (2011).

[5] C. Brune, A. Roth, B. Buhmann, E. M. Hankiewicz, L. W. Molenkamp, J. Maciejko, X.-L. Qi, and S.-C. Zhang, Nat. Phys. **8**, 486 (2012).

[6] A. A. Burkov and D. G. Hawthorn, Phys. Rev. Lett. **105**, 066802 (2010).

[7] M. Büttiker, IBM J. Res. Dev. **32**, 317 (1988).

[8] R. H. Silsbee, J. Phys.: Condens. Matter **16**, R179 (2004).

[9] İ. Adagideli, G. E. W. Bauer, and B. I. Halperin, Phys. Rev. Lett. **97**, 256601 (2006).

[10] D. Culcer, E. H. Hwang, T. D. Stanescu, and S. Das Sarma, Phys. Rev. B **82**, 155457 (2010).

[11] O. V. Yazyev, J. E. Moore, and S. G. Louie, Phys. Rev. Lett. **105**, 266806 (2010).

[12] P. R. Hammar and M. Johnson, Phys. Rev. B **61**, 7207 (2000).

[13] R. H. Silsbee, Phys. Rev. B **63**, 155305 (2001).

[14] P. R. Hammar and M. Johnson, Appl. Phys. Lett. **79**, 2591 (2001).

[15] Y. H. Park, H. Cheol Jang, H. C. Koo, H. Kim, J. Chang, S. H. Han, and H.-J. Choi, J. Appl. Phys. **111**, 07C317 (2012).

[16] R. Stacey, Phys. Rev. D **26**, 468 (1982).

[17] S. Datta, "Nanoelectronic Devices: A Unified View," Chapter 1, vol. I, the *Oxford Handbook on Nanoscience and Nanotechnology*, eds. A. V. Narlikar and Y. Y. Fu (2009), arXiv:0809.4460v2 [cond-mat.mes-hall].

[18] S. Datta, *Electronic Transport in Mesoscopic Systems* (Cambridge University Press, Cambridge, 1997).

[19] Z.-H. Zhu, G. Levy, B. Ludbrook, C. N. Veenstra, J. A. Rosen, R. Comin, D. Wong, P. Dosanjh, A. Ubaldini, P. Syers, N. P. Butch, J. Paglione, I. S. Elfimov, and A. Damascelli, Phys. Rev. Lett. **107**, 186405 (2011).

[20] M. Bianchi, D. Guan, S. Bao, J. Mi, B. B. Iversen, P. D. C. King, and Ph. Hofmann, Nat. Commun. **1**, 128 (2010).

[21] P. D. C. King, R. C. Hatch, M. Bianchi, R. Ovsyannikov, C. Lupulescu, G. Landolt, B. Slomski, J. H. Dil, D. Guan, J. L. Mi, E. D. L. Rienks, J. Fink, A. Lindblad, S. Svensson, S. Bao, G. Balakrishnan, B. B. Iversen, J. Osterwalder, W. Eberhardt, F. Baumberger, and Ph. Hofmann, Phys. Rev. Lett. **107**, 096802 (2011).